A Solid-State ^{13}C NMR Investigation of the Morphology of Single-Site and Ziegler−Natta Linear Low-Density Polyethylenes with Varying Branch Contents

Mingtao Wang,[†,‡] Guy M. Bernard,[‡] Roderick E. Wasylishen,*[,‡] and Phillip Choi*[,†]

Department of Chemical and Materials Engineering, University of Alberta, Edmonton, Alberta, CANADA T6G 2G6, and Department of Chemistry, University of Alberta, Edmonton, Alberta, CANADA T6G 2G2

Received May 17, 2007; Revised Manuscript Received June 27, 2007

ABSTRACT: The morphologies of 1-octene-based linear low-density polyethylenes (LLDPEs) prepared with single-site (ss) or Ziegler−Natta (ZN) catalysts were investigated using solid-state ^{13}C NMR spectroscopy. For each type of LLDPE, two samples, containing either approximately 10 or approximately 30 hexyl branches per 1000 backbone carbons, were studied. Mass fractions of their crystalline and amorphous phases as well as the interphase were quantified; a significant amount of LLDPE exists in the interphase for both types of samples, with their relative amounts decreasing with increasing branch content. Hexyl branches are approximately evenly distributed between the two noncrystalline phases for all samples except the high branch content ZN LLDPE, whose branches tend to cluster in the amorphous phase. The latter observation is attributed to the fact that most of the branched molecules in ZN LLDPE are in the low molar mass fraction and when the branch content is high these chains cannot fold into ordered structural units. The crystalline phase consists of three components with distinct ^{13}C spin−lattice relaxation, T_1, times; the degree of crystallinity decreases with increasing branch content. For samples with similar branch contents, ZN LLDPE tends to have thicker lamellae than does ss LLDPE.

Introduction

With recent advances in catalyst technology, the ability to synthesize polyethylene with a specific architecture has improved significantly. Polyethylene molecules, even in cases where they are chemically similar, may exhibit a wide range of macroscopic properties. For example, the properties of linear low-density polyethylenes (LLDPEs) differ considerably when synthesized using two different catalysts, single site (ss) or Ziegler−Natta (ZN).[1,2] In particular, ss LLDPE exhibits higher dart impact strength than does ZN LLDPE whereas the tear resistance of ZN LLDPE tends to be higher.[1] Also, ZN LLDPE forms thicker lamellae resulting in a melting temperature which is about 10 °C higher than that of ss LLDPE.[3] These observations are attributed to the fact that ZN catalysts tend to incorporate most of the comonomers (i.e., branches) into the low molar mass chains while ss catalysts distribute these evenly into chains of different lengths.[4−9]

For LLDPEs, differences in the distribution of branches among the chains of varying sizes affect the folding of chains into ordered structures which, in turn, leads to differences in the phase structure. Three distinct phases are generally required to characterize polyethylene, the crystalline and amorphous phases as well as an interphase which bridges these two phases.[10−12] Two important questions that have not been addressed in detail are as follows: How are the branches distributed among the three phases? What are the effects of the distribution of branches on the morphological features of the three phases? The former is a fundamental yet not totally resolved problem.[13−16] While methyl, and to some extent ethyl, branches are known to readily incorporate into the crystalline phase, branches containing more than two carbons are essentially excluded from this phase.[13−16] However, the distribution of branches between the two noncrystalline phases of ss and ZN LLDPE prepared under similar crystallization conditions is not known. Does the distribution depend on branch content? In addition, it is not known if the distribution of branches has an effect on the amounts of the two noncrystalline phases. A detailed investigation of these questions is required.

In the work presented here, solid-state ^{13}C NMR spectroscopy was used to investigate low- (∼10) and high- (∼30) branch-content 1-octene-based ss and ZN LLDPE samples. Solid-state NMR spectroscopy is a common technique for investigating the morphology of solid polymers.[17−23] In particular, NMR spectroscopy offers the advantage that local order in noncrystalline phases may be studied, something which cannot be effectively probed by other techniques such as small-angle X-ray or neutron scattering.[17,18] Several methods have been devised to investigate the structure and dynamics of polymers via solid-state NMR, such as proton wide-line NMR[24] and its follow up method, two-dimensional proton wide-line separation (WISE) NMR.[25] In 2D WISE NMR, the ^1H line shapes arising from various sites may be resolved by correlation with the ^{13}C chemical shifts. Another solid-state NMR method is based on the studies of relaxation behavior, including determination of spin−lattice, T_1, and spin−spin, T_2, relaxation times of the nuclei of interest. The relaxation times vary as a function of τ_c, the correlation time.[26,27] A T_1 minimum is induced by molecular motions on the order of the Larmor frequency, usually tens to hundreds of MHz.[26,27] The T_2 relaxation time in solid polymers has a contribution from a frequency-independent term; T_2 values become shorter as τ_c increases.[26,27] The T_1 values of ^{13}C and ^1H nuclei are closely related to the degree of crystallinity and lamellar thickness of polyethylene samples.[28−31] In solid polymer systems, the segmental reorientation and chain diffusion occurring in the

* Corresponding authors. (P.C.) E-mail: phillip.choi@ualberta.ca. Fax: 780 492-2881. Telephone: 780 492-9018. (R.E.W.) E-mail: Roderick.wasylishen@ualberta.ca. Fax: 780 492-8231. Telephone: 780 492-4336.

† Department of Chemical and Materials Engineering, University of Alberta.

‡ Department of Chemistry, University of Alberta.

10.1021/ma071119w CCC: $37.00
Published on Web 08/01/2007

Table 1. Characteristics of LLDPEs Investigated in This Study

sample	M_n[a]	M_w[b]	PDI[c]	density[d]	branch content[e]
ss LLDPE_L	34 800	104 400	3.0	0.9196	11.3
ZN LLDPE_L	26 400	116 160	4.4	0.9229	12.7
ss LLDPE_H	25 700	69 390	2.7	0.902	30.4
ZN LLDPE_H	17 300	105 530	6.1	0.902	35.0

[a] Number-average molar mass, in g mol^{-1}; determined via GPC. [b] Weight-average molar mass, in g mol^{-1}; determined via GPC. [c] Polydispersity index, M_w/M_n. [d] g cm^{-3}; obtained from a flow densitometer method. [e] Number of branches per 1000 backbone carbons; obtained from FTIR measurements calibrated using solution ^{13}C NMR.

noncrystalline phases partially average homonuclear (^{1}H−^{1}H) or heteronuclear (^{1}H−^{13}C) dipole−dipole interactions, resulting in relatively long T_2 values.[32,33] Since the degree of averaging depends on the reorientation rate, evaluation of ^{1}H and ^{13}C T_2 values provides information about phase structure[34−36] and chain dynamics.[37]

In this study, the degree of crystallinity and lamellar thickness as well as the dynamics of the crystalline phases for the samples under consideration were investigated via the analyses of ^{13}C NMR spectra and ^{13}C T_1 relaxation data. Carbon-13 T_2 relaxation processes of relevant sites determined via a modified Hahn-echo pulse sequence[38] (*vide infra*) was used to quantify the amounts of LLDPE in the interphase and to determine the distribution of hexyl branches between the two noncrystalline phases.

Experimental Section

Linear Low-Density Polyethylenes. Four samples of 1-octene-based linear low-density polyethylenes (i.e., LLDPEs with hexyl branches) were obtained from NOVA Chemicals Corp. (Calgary, Canada). Two samples were synthesized using ZN catalysts while the other two were synthesized by ss catalysis. The characteristics of the samples, listed in Table 1, show that they possess two levels of branch contents: approximately 10 or 30 hexyl branches per 1000 backbone carbons, hereinafter referred to as low (LLDPE_L) or high (LLDPE_H) branch-content materials, respectively.

Solid-State ^{13}C NMR. Solid-state ^{13}C NMR spectra were acquired using a Chemagnetics CMX Infinity 200 spectrometer, operating at approximately 200.15 MHz for ^{1}H and 50.32 MHz for ^{13}C. Samples were packed in 7.5 mm o.d. zirconia rotors. ^{13}C NMR spectra of ss and ZN LLDPE samples were obtained with cross-polarization and magic angle spinning (CP/MAS) at room temperature with a spinning frequency of 3.00 kHz. The ^{1}H 90° pulse was 4.5 μs and the contact time was 1 ms. Since spectra obtained with CP are not quantitative, ^{13}C NMR spectra of ss and ZN LLDPEs were also acquired with single-pulse excitation, SPE, using a ^{13}C 90° pulse of 4.5 μs and a 1500 s recycle delay to ensure complete relaxation of the ^{13}C nuclei. The two-pulse phase modulation (TPPM) scheme[39] was used for ^{1}H decoupling for all ^{13}C NMR spectra; these spectra were referenced to tetramethylsilane (Me_4Si, $\delta_{iso} = 0$) by setting the isotropic high-frequency peak of adamantane to 38.56 ppm.[40] The ^{13}C T_1s of the crystalline phase of the samples were measured via CP using the pulse sequence reported by Torchia[41] (hereinafter referred to as the CPT_1 pulse sequence). The ^{13}C T_2s of the noncrystalline phases of the samples were estimated using a modified Hahn-echo pulse sequence (90°-τ-180°-τ-ACQ) suggested by Kitamaru et al.,[36] referred to herein as the T_2 pulse sequence, in which ^{1}H decoupling was delayed until acquisition of the FID; because T_1 values of these noncrystalline phases are short (≤1 s), CP was not used. The decay of the transverse magnetization of the backbone methylene carbons in the noncrystalline region was fit to exponential decay functions containing adjustable parameters, from which the quantity of the associated components could be calculated. The partitioning of hexyl branches between the interphase and amorphous phase was also investigated using the T_2 data from the **5** carbons (Figure 1).

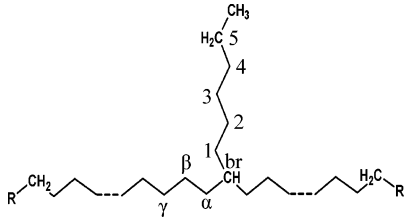

Figure 1. Numbering scheme and abbreviations for the carbon atoms of LLDPE. The carbon at the branching site is designated br; the backbone carbons are labeled α, *β*, *γ*, ..., where α is the carbon bonded to the br carbon; the branch carbons are designated 1, 2, 3, ..., where 1 is the carbon bonded to the br carbon. The backbone ends are represented by R.

Gel Permeation Chromatography (GPC) Measurements of Fuming Nitric Acid (FNA) Etched Samples. The low-branch content samples were immersed in sealed glass bottles that contained FNA and placed in an oil bath at 60 °C (the high branch-content samples were not subjected to FNA etching). The samples were allowed to degrade for 1, 2, or 30 days. After etching, the residue of each sample was filtered and washed several times with distilled water and then immersed in distilled water and rinsed for 24 h. The cleansed samples were then dried overnight in a vacuum oven at room temperature. GPC measurements were used to determine the molar mass as well as the mass distribution of the samples subjected to different etching conditions. These measurements were performed at 145 °C on an Alliance GPCV 2000 using 1,2,4-trichlorobenzene as the solvent and Waters HT6E columns with guard coils. The flow rate for the GPC measurements was 1.0 mL/min. Linear polyethylene samples with a narrow molecular weight distribution were used as calibration standards. The data for the 30-day etched LLDPEs were used to calculate the lamellar thickness.

Results and Discussion

Carbon-13 NMR Peak Assignments. Carbon-13 NMR spectra of low- and high-branch content ss and ZN LLDPEs were obtained with MAS using either CP or SPE at room temperature. Figure 2 illustrates ^{13}C NMR spectra for ss LLDPE_L (a and b) and ss LLDPE_H (c and d); those for the ZN type are similar. An intense sharp peak at 32.9 ppm and another intense but broader peak at approximately 31.0 ppm are present in all spectra. Since the value of 32.9 ppm corresponds to the isotropic chemical shift of trans−trans methylene sequences of polyethylene in the orthorhombic crystalline form,[42,43] this peak is assigned to the crystalline phase. The value of 31.0 ppm is close to that reported for melted polyethylene samples[44,45] and is attributed to the noncrystalline phases. The width of this peak is a consequence of the fact that a range of conformations exist in the noncrystalline phases which give rise to a set of conformation-dependent resonance frequencies.[46] The mass fractions of the crystalline and noncrystalline phases of the LLDPEs were determined through the deconvolution of the two peaks at 32.9 and 31.0 ppm from spectra acquired with SPE; the results are summarized in Table 2. In addition to the two intense peaks, smaller peaks at 38.4, 27.4, 23.8, and 15.1 ppm are apparent (Figure 2d); based on solution NMR studies,[44,45] these are assigned to the br, *β*, **5**, and methyl carbons (Figure 1), respectively. For spectra acquired with SPE, the integrated intensities of the peaks of the **5** carbons and the methyl carbons are approximately the same. The data show that the degree of crystallinity decreases with increasing branch content, which is expected since the branches disrupt the formation of lamellae.[47,48]

Carbon-13 NMR spectra of ss LLPDE_L and LLDPE_H, recorded using the T_2 pulse sequence, are shown in Figure 3,

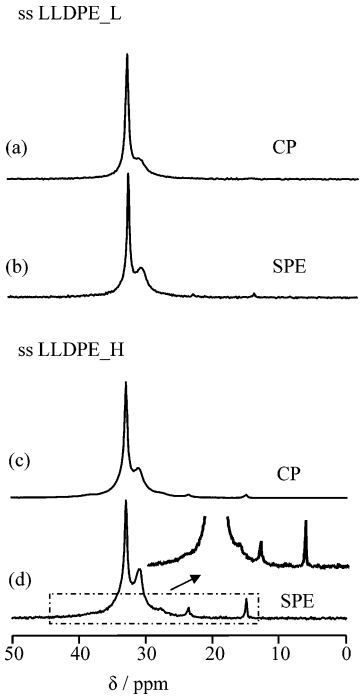

Figure 2. Carbon-13 NMR spectra of MAS samples of (a) ss LLDPE_L acquired with CP and (b) with SPE, and (c) of ss LLDPE_H acquired with CP and (d) with SPE. Spectra were acquired at a spinning frequency of 3.00 kHz.

Table 2. Parameters Obtained for ss and ZN LLDPE, with Low and High Branch Content

sample	T_1/s	T_2/ms	mass fraction
ss LLDPE_L			
crystalline	202 ± 12		0.41 ± 0.02
	35.5 ± 4		
	1.1 ± 0.1[a]		
interfacial		0.064 ± 0.006	0.48 ± 0.03
amorphous		2.1 ± 0.9	0.11 ± 0.03
ZN LLDPE_L			
crystalline	237 ± 14		0.48 ± 0.02
	22.6 ± 3		
	1.0 ± 0.1[a]		
interfacial		0.072 ± 0.006	0.40 ± 0.03
amorphous		2.4 ± 0.9	0.12 ± 0.03
ss LLDPE_H			
crystalline	136 ± 5		0.27 ± 0.02
	14.6 ± 2		
	0.65 ± 0.08[a]		
interfacial		0.065 ± 0.009	0.51 ± 0.03
amorphous		3.3 ± 0.9	0.22 ± 0.03
ZN LLDPE_H			
crystalline	154 ± 6		0.26 ± 0.02
	16.1 ± 2		
	0.63 ± 0.09[a]		
interfacial		0.070 ± 0.01	0.48 ± 0.03
amorphous		2.4 ± 0.9	0.26 ± 0.03

[a] See text for a discussion of the nature of this component.

parts a and b, respectively; the crystalline peaks are suppressed because of the relatively short recycle delay time, 5 s. Although the peak of 23.8 ppm may have contributions from backbone CH_2 carbons, based on M_w and the branch content for the samples of interest, over 97% of the intensity of the peak is estimated to come from the **5** carbons in the branches for all four samples; hence, contributions from other carbons to this peak are assumed to be negligible.

The Crystalline Phase. The structural features and dynamics of the crystalline phase were investigated via a T_1 relaxation study of the ^{13}C nuclei in this phase. Figure 4 shows the relaxation of the longitudinal magnetization of the crystalline

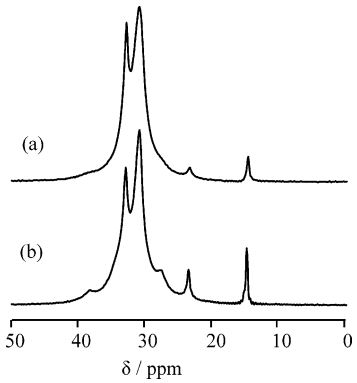

Figure 3. Carbon-13 NMR spectra of MAS samples of (a) ss LLDPE_L and (b) ss LLDPE_H acquired using a modified Hahn-echo pulse sequence with $\tau = 25$ μs and a recycle delay of 5 s. Spectra were acquired at a spinning frequency of 3.00 kHz.

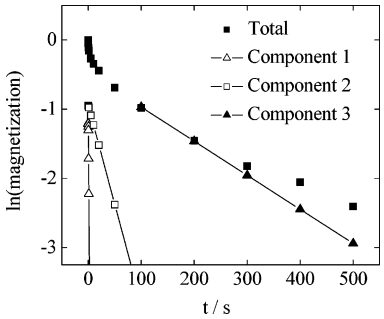

Figure 4. Measurement of the ^{13}C spin−lattice relaxation for the crystalline phase of ss LLDPE_L: ln(magnetization) vs time. For the fit, $R^2 = 0.999$, $\chi^2/\mathrm{DoF} = 0.0002$.

phase of ss LLDPE_L, measured with the CPT_1 pulse sequence.[41] Similar relaxation curves were obtained for the other three LLDPE samples considered here. As reported for other polyethylene samples,[34,36] the curve cannot be fit to a single-exponential decay function. In fact, the data were resolved into three components with T_1 values and magnetization weights determined by best fits of the data to[41]

$$M_{\mathrm{total}}(t) = M_{\mathrm{a}}(0)\exp(-t/T_{1\mathrm{a}}) + M_{\mathrm{b}}(0)\exp(-t/T_{1\mathrm{b}}) + M_{\mathrm{c}}(0)\exp(-t/T_{1\mathrm{c}}) \quad (1)$$

where $M_{\mathrm{total}}(t)$ is the total longitudinal magnetization of the crystalline components at time t and $M_{\mathrm{i}}(0)$ (i = a, b, or c) is the initial magnetization of the constituent component with spin−lattice relaxation time, $T_{1\mathrm{i}}$.

As determined from fits of the relaxation data to eq 1, each sample contains components of the peak at 32.9 ppm with short (≈1 s), intermediate (15−35 s), and long (135−235 s) T_1s; see Table 2. Approximately 60% of the magnetization for the peak at 32.9 ppm for each sample arises from the component with the long T_1s, 30% from that with the intermediate value and 10% from that with the short T_1. These data were obtained from a CP experiment; hence further quantification of the crystalline component into mass fractions for components with different T_1s is not possible since we cannot be certain that these components have the same CP dynamics. Nevertheless, the data indicate that a significant fraction of the samples have crystalline components with T_1s on the order of 1 s; this is surprising since crystals generally do not have a mechanism for such rapid ^{13}C relaxation. Several explanations have been offered for this anomalous behavior which has been observed previously.[36,49,50,51] Kitamuru and co-workers suggested that segments in the crystalline phase that are either close to the interface, or that

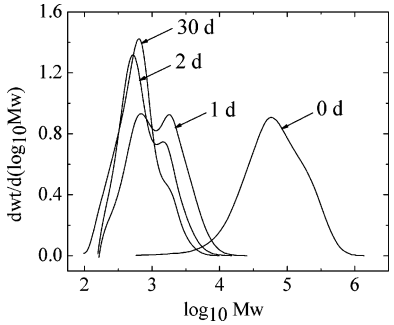

Figure 5. Gel permeation chromatograms of ss LLDPE_L samples subjected to different FNA etching times.

are in thin or defective lamellae, have T_1s of approximately1 s.[36] Chain diffusion between the crystalline and noncrystalline phases of polyethylene samples has also been proposed as an explanation for the low T_1 values.[49,50] Recently, Chaiyut et al. reported ^{13}C T_1 values ranging from 0.9 to 1.39 s for a peak at 33.3 ppm, arising from a noncrystalline component of a highly drawn polyethylene which has an all-trans conformation but lacks lateral order.[51] Since this chemical shift is close to that of the crystalline components for the samples considered here, a similar noncrystalline component could be responsible for the short T_1 values that we are observing. Two orthorhombic crystalline components with distinct dynamics have been reported for polyethylene; these may give rise to the intermediate and long T_1s observed for our samples.[52,53] However, Schmidt-Rohr et al.[54] recently suggested that all-trans chains for cold-drawn high-density polyethylene with disordered packing have a chemical shift of ~33 ppm and intermediate ^{13}C T_1 values. The component with the greatest T_1 value has been attributed to the core of the larger lamellae.

Since ^{13}C T_1 values for the crystalline phase are an indication of its lamellar thickness,[28,49] these may be used to gain insight into the thickness of the lamellae for the samples considered here. Comparison of the longest T_1 values for each sample (Table 2) suggests that, with similar branch contents, ZN LLDPE has thicker lamellae than does ss LLDPE. The T_1 data also suggest that the lamellar thickness decreases with increasing branch content, which is expected since increasing the branch concentration impedes the growth of lamellae.[47,48] To corroborate the T_1 data, GPC measurements of FNA etched ss and ZN LLDPE_L samples were performed. Under appropriate conditions, FNA selectively removes the noncrystalline phases while leaving the crystallites undamaged.[55−58] Figure 5 shows the molar mass distribution curves of ss LLDPE_L subjected to periods of FNA etching (a comparable GPC result was obtained for ZN LLDPE_L). The corresponding average lamellar thickness was calculated based on the following assumptions: all carbons in the lamellar stems are in the *trans* form, the C−C bond length is 1.534 Å and the C−C−C bond angle is approximately 110 degrees.[59,60] The number of CH_2 units in the lamellar stems was calculated by dividing the average molar mass, obtained from the GPC measurements, by the molar mass of the CH_2 unit. The results, summarized in Table 3, suggest that 30 days is sufficient to remove the noncrystalline phases of the materials without damaging the lamellar stems. Removal of the noncrystalline phases was confirmed by ^{13}C CP/MAS NMR spectra of samples that had been FNA etched for 30 days (not shown). T_1 measurements of the 30-day etched samples confirm the presence of the three components discussed above. As shown in Table 3, the average lamellar thickness of ZN LLDPE_L is greater than that of ss LLDPE_L, consistent with the conclusions drawn from an analysis of the T_1 data, discussed above.

Table 3. Average Molar Mass and Corresponding Crystal Lengths for ss and ZN LLDPEs after FNA Etching[a,b]

sample	t_e/days	M_n/g mol^{-1}	M_w/g mol^{-1}	PDI	L_n/Å	L_w/Å
ss LLDPE_L	1	831	1692	2.04	75	152
	2	576	1030	1.79	52	92
	30	474	812	1.71	43	73
ZN LLDPE_L	1	1147	2596	2.26	103	233
	2	609	1096	1.80	55	98
	30	505	912	1.78	45	82

[a] t_e is the experiment time; L_n and L_w are the number-average length and weight-average length, respectively. See the footnotes to Table 1 for an explanation of the other terms used in this table. [b] Data are considered accurate to within 10%.

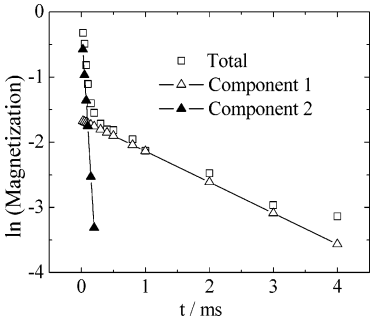

Figure 6. Measurement of the ^{13}C spin−spin relaxation for the noncrystalline phases of ss LLDPE_L: ln(magnetization) vs time. For the fit, $R^2 = 0.995$, $\chi^2/\text{DoF} = 0.0003$.

The Crystalline−Amorphous Interphase. Defining the spatial boundaries of the interphase can be difficult. However, at the temperature used to acquire NMR data here, $T = 20$ °C, which is between the glass transition temperature and the melting point of polyethylene, molecular motions such as rotation (segmental) in the interphase are much less than those in the amorphous phase. Since the effective dipole−dipole interaction between ^{13}C and ^{1}H nuclei decreases with increased molecular motion, the interphase is expected to experience stronger effective $^{13}C-^{1}H$ dipolar interactions than those in the amorphous phase; this in turn results in shorter spin−spin relaxation times for the former. Thus, a room temperature T_2 study of the peak arising from the noncrystalline phases allows one to differentiate between the two phases. Figure 6 shows the ^{13}C T_2 relaxation behavior of the noncrystalline phases of ss LLDPE_L. Two components with distinct T_2 values were required to fit the decay:

$$M_{ytotal}(t) = M_{yI}(0)\exp(-t/T_{2I}) + M_{yA}(0)\exp(-t/T_{2A}) \quad (2)$$

where $M_{ytotal}(t)$ is the total transverse magnetization of the noncrystalline phases at time t, and $M_{yI}(0)$, $M_{yA}(0)$ are the respective transverse magnetization at time $t = 0$ of the interphase and amorphous phase. These are proportional to the quantity of the two phases provided the recycle delay in the experiments is sufficiently long (i.e., $\geq 5T_1$). The T_2 values measured here are listed in Table 2. The fact that the measured transverse magnetizations are best fit by two T_2 values that differ by 2 orders of magnitude confirms that molecular motions in the interphase are different from those in the amorphous phase. For a polymer chain, segmental motions have a range of τ_c^{-1} values: high frequencies for short segments that may contain less than 10 monomer units; low frequencies for long segments that have long-range motions.[61] The short segment high-frequency motions may be similar for the interphase and the

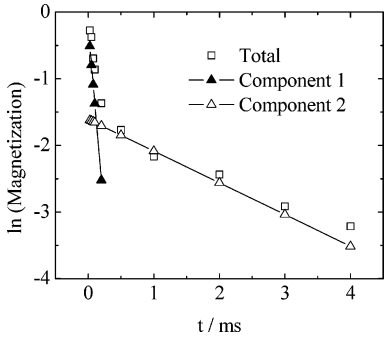

Figure 7. Measurement of the spin−spin relaxation time for the **5** ^{13}C nuclei of ss LLDPE_L: ln(magnetization) vs time. For the fit, $R^2 = 0.994$, $\chi^2/\text{DoF} = 0.0002$.

amorphous phase of LLDPEs, as suggested by the similar T_1 values of these two phases.[34,36] However, the long segment low-frequency motions in the interphase are expected to be much less than those in the amorphous phase.

The mass fractions of the noncrystalline phases were calculated based on the degree of crystallinity obtained from the deconvolution of the ^{13}C NMR spectra of MAS samples, and on the M_{yI} and M_{yA} values. The data show that all four LLDPEs contain a relatively large mass fraction of interphase. This observation is consistent with previous reports. For example, Raman analysis and X-ray diffraction studies show that approximately 20−30% of high-density polyethylene samples are in the interphase.[12,62] Also using solid-state ^{13}C NMR, Kuwabara et al.[34] showed that 40−50% of metallocene-catalyzed and ZN LLDPE samples are in the interphase. The large mass fraction of the interphase is attributable to a strong restriction imposed by the crystalline lamellae on the conformational dynamics of the noncrystalline phases; the amount of interphase indicates that the restriction is extensive and that only after a significant distance are the noncrystalline phases random and mobile. For a given LLDPE type (either ZN or ss), the amount of interphase for the low branch-content sample is approximately the same as that of its high branch-content counterpart over the branch-content range studied. However, as expected, the amount of the amorphous phase increases with increasing branch content; at the limit of very high branch content, the material is expected to be completely amorphous.

Concentration of Hexyl Branches in the Three Phases. Other workers[13,14,16] have shown that branches with more than two carbons are excluded from the crystalline phase and thus are distributed between the two noncrystalline phases. The mobility of the carbons of the hexyl branches depends on the phase in which they reside; determination of the T_2 values for one of the branch ^{13}C nuclei, therefore, allows one to distinguish between branches located in the two noncrystalline phases. In their investigation of low branch-content metallocene-catalyzed and ZN LLDPEs, Kuwabara et al.[34] determined the partitioning of butyl branches between the interphase and the amorphous phase through the measurement of the T_2 relaxation of the methine carbons. As seen in Figure 3, the peak at 23.8 ppm, attributed to the **5** carbons, is more suitable for an investigation of the relaxation behavior of the samples considered here, since it is relatively intense and it is isolated from the intense peaks arising from the backbone carbons. The peak assigned to the methyl carbons at 15.1 ppm is not suitable because this group is subject to significant motion regardless of the phase in which it resides.

Figure 7 illustrates that two distinct components are required to describe the T_2 relaxation of the **5** carbons giving rise to the peak at 23.8 ppm. The component with the shorter T_2 value is from nuclei located in the interphase; the one with the longer T_2 value is attributed to nuclei in the amorphous phase. The T_2 values and the fractions of these two components, determined from fits of the observed data, are summarized in Table 4. One may expect that the T_2 values of the **5** carbons would be different from those of the noncrystalline backbone carbons since the former may have more reorientational freedom; however, these values are in fact similar. The concentrations of the branches in the two noncrystalline phases and the overall branch concentrations were determined using the information in Tables 2 and 4 as well as the relative integrated intensities of the NMR peaks of the **5** carbons and the noncrystalline backbone carbons, which were obtained with the T_2 pulse sequence; the results are shown in Table 5. The predicted overall branch concentrations are consistent with those listed in Table 1. Note that addition of branches decreases the relative amount of interphase in an LLDPE sample but not its absolute amount. The data clearly indicate that, at low branch contents, branches are approximately evenly distributed between the interphase and the amorphous phase for both types of LLDPEs. This conclusion is in agreement with that reached by Kuwabara and co-workers for metallocene-catalyzed and ZN LLDPEs.[34] However, at high branch content, ZN LLDPE shows an imbalanced distribution with a greater portion of the branches clustering in the amorphous phase. This is expected since branches in ZN LLDPE tend to originate from the low molar mass fraction and when the concentration is high these chains cannot crystallize. However, this is not the case for high branch content ss LLDPE, which has a nearly homogeneous branch distribution between the interphase and the amorphous phase. This finding is consistent with the molecular dynamics simulation results of Zhang et al.[63]

Table 4. T_2 Values and Fractions of the 5 Carbons

	T_2/ms	fraction/%
ss LLDPE_L		
interfacial	0.087 ± 0.01	80 ± 9
amorphous	2.3 ± 1.0	20 ± 2
ZN LLDPE_L		
interfacial	0.074 ± 0.01	75 ± 7
amorphous	3.4 ± 0.8	25 ± 3
ss LLDPE_H		
interfacial	0.068 ± 0.01	72 ± 7
amorphous	4.4 ± 1.2	28 ± 3
ZN LLDPE_H		
interfacial	0.092 ± 0.01	50 ± 6
amorphous	5.4 ± 1.1	50 ± 6

Table 5. Branch Concentrations of the Two Noncrystalline Phases of ss and ZN LLDPE

	concentration[a]	
phase	ss LLDPE_L	ss LLDPE_H
interfacial	21.4 ± 2.5	50.7 ± 7.5
amorphous	22.7 ± 2.5	45.5 ± 6.6
overall	12.8 ± 1.5	35.9 ± 5.2

	concentration[a]	
phase	ZN LLDPE_L	ZN LLDPE_H
interfacial	23.8 ± 2.7	41.8 ± 6.1
amorphous	26.7 ± 3.0	77.1 ± 10.9
overall	12.7 ± 1.5	40.1 ± 5.7

[a] The interfacial or amorphous concentration is expressed as number of branches per 1000 backbone carbons of the corresponding phase; the overall branch concentration is expressed as number of branches per 1000 backbone carbons.

Conclusions

The crystalline and noncrystalline phases of single site and Ziegler−Natta LLDPEs, each with both ∼10 and ∼30 branches per 1000 backbone carbons, have been investigated using solid-state ^{13}C NMR spectroscopy. A significant amount of LLDPE exists in the interphase for both types of LLDPEs. Although increasing the branch content does not change the absolute amount of the interphase, it does decrease the relative amount of this phase, normalized against the total noncrystalline fraction. Hexyl branches are evenly distributed between the interphase and the amorphous phase for both types of LLDPEs with the lower level of branch content; however at higher levels of branch content, hexyl branches are denser in the amorphous phase than in the interphase for ZN LLDPE but are nearly homogenously distributed between these two phases for ss LLDPE. The degree of crystallinity decreases with increasing branch content. The peak attributed to the crystalline phase is the sum of components with three distinct T_1 values. ZN LLDPE tends to have thicker lamellae than does the corresponding ss LLDPE sample with similar branch content.

Acknowledgment. The authors thank members of the solid-state NMR group at the University of Alberta for many helpful comments in the preparation of this manuscript. We acknowledge the generous financial support of NOVA Chemicals Corporation and the Natural Sciences and Engineering Research Council of Canada through a collaborative research grant. M.W. and P.C. thank the research group at NOVA Research and Technology Centre for many stimulating discussions. R.E.W. thanks the Government of Canada for the Canada Research Chair in Physical Chemistry at the University of Alberta.

References and Notes

(1) Guichon, O.; Seguela, R.; David, L.; Vigier, G. *J. Polym. Sci., Part B: Polym. Phys.* **2003**, *41*, 327−340.
(2) ChuU, K.-J.; Ha, J.-W.; Park, T.-H. *Mater. Lett.* **1997**, *30*, 115−121.
(3) Shanks, R. A.; Amarasinghe, G. *J. Therm. Anal. Cal.* **2000**, *59*, 471−482.
(4) Mirabella, F. M.; Ford, E. A. *J. Polym. Sci., Part B: Polym. Phys.* **1987**, *25*, 777−790.
(5) Wild, L. *Adv. Polym. Sci.* **1990**, *98*, 1−47.
(6) Adisson, E.; Ribeiro, M.; Deffieux, A.; Fontanille, M. *Polymer* **1992**, *33*, 4337−4342.
(7) Mirabella, F. M. *J. Polym. Sci., Part B: Polym. Phys.* **2001**, *39*, 2800−2807.
(8) Wolf, B.; Kenig, S.; Klopstock, J.; Miltz, J. *J. Appl. Polym. Sci.* **1996**, *62*, 1339−1345.
(9) Monrabal, B. *J. Appl. Polym. Sci.* **1994**, *52*, 491−502.
(10) Flory, P. J. *J. Am. Chem. Soc.***1962**, *84*, 2857−2867.
(11) Mandelkern, L. *Acc. Chem. Res.* **1990**, *23*, 380−389.
(12) Wunderlich, B. *Prog. Polym. Sci.* **2003**, *28*, 383−450.
(13) Perez, E.; VanderHart, D. L.; Crist, B., Jr.; Howard, P. R. *Macromolecules* **1987**, *20*, 78−87.
(14) VanderHart, D. L.; Perez, E. *Macromolecules* **1986**, *19*, 1902−1909.
(15) Balta Calleja, F. J.; Hosemann, R. *J. Polym. Sci., Polym. Phys. Ed.* **1980**, *18*, 1159−1172.
(16) Chen, J.; Fone, M.; Reddy, V. N.; Schwartz, K. B.; Fisher, P. H.; Wunderlich, B. *J. Polym. Sci., Part B: Polym. Phys.* **1994**, *32*, 2683−2693.
(17) Spiess, H. W. *J. Polym. Sci., Part A: Polym. Chem.* **2004**, *42*, 5031−5044.
(18) Schmidt-Rohr, K.; Spiess, H. W. *Multidimensional Solid-State NMR and Polymers*; Academic Press: San Diego, CA, 1994.
(19) Spiess, H. W. *Macromol. Chem. Phys.* **2003**, *204*, 340−346.
(20) Spiess, H. W. *Annu. Rep. NMR Spectrosc.* **1997**, *34*, 1−37.
(21) Hedesiu, C.; Demco, D. E.; Kleppinger, R.; Buda, A. A.; Blümich, B.; Remerie, K.; Litvinov, V. M. *Polymer* **2007**, *48*, 763−777.
(22) Horii, F.; Kaji, H.; Ishida, H.; Kuwabara, K.; Masuda, K.; Tai, T. *J. Mol. Struct.* **1998**, *441*, 303−311.
(23) Klein, P. G.; Driver, M. A. *Macromolecules* **2002**, *35*, 6598−6612.
(24) Bergmann, K. *J. Polym. Sci.: Polym. Phys. Ed.* **1978**, *16*, 1611−1634.
(25) Schmidt-Rohr, K.; Clauss, J.; Spiess, H. W. *Macromolecules* **1992**, *25*, 3273−3277.
(26) Harris, R. K. *Nuclear Magnetic Resonance Spectroscopy−A Physicochemical View;* Longman: Harlow, UK, **1986.**
(27) Ward, I. M.; Klein, P. G. In *Encyclopedia of Nuclear Magnetic Resonance*; Grant, D. M.; Harris, R. K.; Eds.; John Wiley & Sons: Chichester, England, 1996; Vol. 6, pp 3693−3706.
(28) Axelson, D. E.; Mandelkern, L.; Popli, R.; Mathieu, P. *J. Polym. Sci., Polym. Phys. Ed.* **1983**, *21*, 2319−2335.
(29) Hong, K.; Ströbl, G. *Macromolecules* **2006**, *39*, 268−273.
(30) English, A. D. *Macromolecules* **1984**, *17*, 2182−2190.
(31) Packer, K. J.; Pope, J. M.; Yeung, R. R.; Cudby, M. E. A. *J. Polym. Sci. Polym. Phys.* **1984**, *22*, 589−596.
(32) Stringfellow, T. C.; Farrar, T. C. *Conc. Magn. Reson.* **1998**, *10*, 261−273.
(33) Fyfe, C. A. *Solid State NMR for Chemists*; C.F.C. Press: Guelph, Ontario, Canada, 1983.
(34) Kuwabara, K.; Kaji, H.; Horii, F.; Bassett, D. C.; Olley, R. H. *Macromolecules* **1997**, *30*, 7516−7521.
(35) Shimizu, Y.; Harashina, Y.; Sugiura, Y.; Matsuo, M. *Macromolecules* **1995**, *28*, 6889−6901.
(36) Kitamaru, R.; Horii, F.; Murayama, K. *Macromolecules* **1986**, *19*, 636−643.
(37) Leisen, J.; Beckham, H. W.; Sharaf, M. A. *Macromolecules* **2004**, *37*, 8028−8034.
(38) Hahn, E. L. *Phys. Rev.* **1950**, *80*, 580−594.
(39) Bennett, A. E.; Rienstra, C. M.; Auger, M.; Lakshmi, K. V.; Griffin, R. G. *J. Chem. Phys.* **1995**, *103*, 6951−6958.
(40) Earl, W. L.; VanderHart, D. L. *J. Magn. Reson.* **1982**, *48*, 35−42.
(41) Torchia, D. A. *J. Magn. Reson.* **1978**, *30*, 613−616.
(42) VanderHart, D. L. *J. Chem. Phys.* **1976**, *64*, 830−834.
(43) Earl, W. L.; VanderHart, D. L. *Macromolecules* **1979**, *12*, 762−767.
(44) Axelson, D. E.; Levy, G. C.; Mandelkern, L. *Macromolecules* **1979**, *12*, 41−52.
(45) Usami, T.; Takayama, S. *Macromolecules* **1984**, *17*, 1756−1761.
(46) Born, R.; Spiess, H. W. *Ab Initio Calculations of Conformational Effects on ^{13}C NMR Spectra of Amorphous Polymers*; Springer: New York, 1997.
(47) Alamo, R. G.; Viers, B. D.; Mandelkern, L. *Macromolecules* **1993**, *26*, 5740−5747.
(48) Zhang, X.-B.; Li, Z.-S.; Yang, H.; Sun, C.-C. *Macromolecules* **2004**, *37*, 7393−7400.
(49) Schmidt-Rohr, K.; Spiess, H. W. *Macromolecules* **1991**, *24*, 5288−5293.
(50) Hu, J. Z.; Wang, W.; Bai, S.; Pugmire, R. J.; Taylor, M. V.; Grant, D. M. *Macromolecules* **2000**, *33*, 3359−3367.
(51) Chaiyut, N.; Amornsakchai, T.; Kaji, H.; Horii, F. *Polymer* **2006**, *47*, 2470−2481.
(52) Hillebrand, L.; Schmidt, A.; Bolz, A.; Hess, M.; Veeman, M.; Meier, R. J. *Macromolecules* **1998**, *31*, 5010−5021.
(53) Kuwabara, K.; Kaji, H.; Tsuji, M.; Horii, F. *Macromolecules* **2000**, *33*, 7093−7100.
(54) Mowery, D. M.; Harris, D. J.; Schmidt-Rohr, K. *Macromolecules* **2006**, *39*, 2856−2865.
(55) Capaccio, G.; Ward, I. M. *J. Polym. Sci.: Polym. Phys. Ed.* **1981**, *19*, 667−679.
(56) Capaccio, G.; Ward, I. M. *J. Polym. Sci.: Polym. Phys. Ed.* **1982**, *20*, 1107−1117.
(57) Pascale, J. V.; Rentzepis, P. M. *J. Appl. Polym. Sci.* **1965**, *9*, 2641−2655.
(58) Uehara, A.; Aoike, T.; Yamanobe, T.; Komoto, T. *Macromolecules* **2002**, *35*, 2640−2647.
(59) Miao, M. S.; Van Camp, P. E.; Van Doren, V. E.; Ladik, J. J.; Mintmire, J. W. *Phys. Rev. B* **1996**, *54*, 10430−10435.
(60) Montanari, B.; Ballone, P.; Jones, R. O. *J. Chem. Phys.* **1998**, *108*, 6947−6951.
(61) Cohen-Addad, J. P.; Dupeyre, R. *Polymer* **1983**, *24*, 400−408.
(62) Cheng, J.; Fone, M.; Reddy, V. N.; Schwartz, K. B.; Fisher, H. P.; Wunderlich, B. *J. Polym. Sci., Part B: Polym. Phys.* **1994**, *32*, 2683−2693.
(63) Zhang, M.; Yuen, F.; Choi, P. *Macromolecules* **2006**, *39*, 8517−8527.

MA071119W